

J. Phys. Chem. C, 117(2), 1146-1150 (2013)

DOI: 10.1021/jp3091478

The transport of mass at the nano-scale during evaporation of droplets: the Hertz-Knudsen equation at the nano-scale

Marcin Zientara,^{*,†} Daniel Jakubczyk,[†] Marek Litniewski,[‡] and Robert Holyst[‡]

Institute of Physics of the Polish Academy of Sciences, al. Lotników 32/46, 02-668 Warsaw, Poland, and Institute of Physical Chemistry of the Polish Academy of Sciences, Kasprzaka 44/52, 01-224 Warsaw, Poland

E-mail: zientara@ifpan.edu.pl

Abstract

The applicability of Hertz-Knudsen equation to evolution of droplets at the nano-scale was investigated upon analysis of existing molecular dynamics (MD) simulations [Holyst *et al.*, *PRL* **100**; Yaguchi *et al.*, *J. Fluid. Sci. Tech.* **5**; Ishiyama *et al.*, *Phys. Fluids* **16**]. The equation was found satisfactory for radii larger than ~ 4 nm. Concepts of Gibbs equimolecular dividing surface and the surface of tension were utilized in order to accommodate the surface phase density and temperature profiles, clearly manifesting at the nano-scale. The equimolecular dividing surface was identified as the surface of the droplet. A modification to the Tolman formula was proposed in order to describe surface tension for droplet radii smaller than ~ 50 nm. We assumed that the evaporation coefficient for a system in and out of equilibrium may differ. We verified that this difference might be attributed to surface temperature change

*To whom correspondence should be addressed

[†]Institute of Physics of the Polish Academy of Sciences

[‡]Institute of Physical Chemistry of the Polish Academy of Sciences

1
2
3 only. The empirical dependencies of the evaporation coefficient and the surface tension for flat
4 interface, of liquid Ar in Ar gas at equilibrium, at the nano-scale, upon temperature was taken
5 from existing MD data. Two parameterizations of the Hertz-Knudsen equation were proposed:
6
7 (i) one using off-equilibrium condensation coefficient and effective density and (ii) another
8 one using effective density and temperature at the interface. The second parametrization leads
9 to an approximate solution of the Hertz-Knudsen equation requiring no free parameters. Such
10 solution is suitable for experimental use at the nano-scale if only the temperature of the droplet
11 (core) can be measured.
12
13
14
15
16
17
18

19
20 **Keywords:** nano-droplet evaporation/condensation, Hertz-Knudsen equation, condensation
21 coefficient.
22
23

24 25 26 Introduction

27
28
29 The ubiquitous processes of evaporation and condensation arouse continued interest. A detailed
30 modeling of these processes, especially concerning evaporation of droplets, is of interest, because
31 of their role in the Earth ecosystem and in technology. Molecular dynamics (MD) simulations¹
32 provide valuable data on these processes. However, the large scale, engineering applications of
33 MD is still far from being feasible, while it seems that the continuous-medium descriptions of
34 evaporation/condensation can provide many valuable information even at the sub-micro-scale (see
35 eg.^{2,3}).

36
37 In this work, we examine the extent of applicability of the (kinetic theory of gases) Hertz-
38 Knudsen (HK) model^{4,5} to nano-scale evaporation. We used available in literature MD data^{6,8,9} to
39 test our hypotheses.
40
41
42

43
44 The HK model considers free, ballistic motion of vapor particles near the droplet surface and
45 introduces the permeability of the gas-liquid interface to these particles in a form of the accommo-
46 dation (evaporation, condensation) coefficient as an empirical parameter. The HK model utilizes
47 the concept of geometrical droplet radius and well localized (bulk) physical properties such as
48 surface tension or density. It works well enough at the micro-scale though may not be sufficient
49
50
51
52
53
54
55
56
57
58
59
60

to describe droplet evaporation/condensation at the nano-scale where sharp boundaries are lost. The surface region is discernible at the nano-scale (see figure 1) while it would be invisible at the micro-scale. If the HK model is to be adapted to the nano-scale, it is necessary to (re)define a few fundamental concepts: where the surface of the droplet is located, where the surface tension is exerted, which values from the density and temperature profiles should be used in transport equations, etc. Similarly, the applicability of the Antoine, Kelvin and Tolman equations at the nano-scale must be verified.

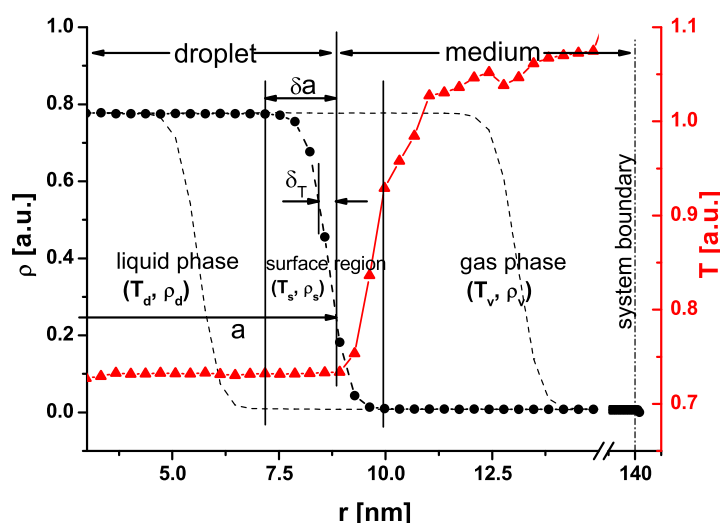


Figure 1: Fluid density profiles for various stages of nano-droplet evaporation (MD simulation from⁶) shown as solid dots and dashed lines. Middle stage (solid dots) accompanied by the corresponding temperature profile ((red) solid triangles and solid line).

We used concepts of the Gibbs equimolecular dividing surface and the surface of tension (see eg.¹⁰). They were introduced by Gibbs and developed independently by Tolman and Koenig, who derived approximate formulas linking the positions of these surfaces.^{11,12} The equimolecular (equimolar) dividing surface is a boundary in a hypothetical system of equal total number of molecules, at which the density changes discontinuously from liquid to vapor.¹⁰ The surface of tension is defined as the surface for which the Laplace equation holds exactly for all droplet radii. The equimolecular dividing surface was identified as the surface of the droplet and was used as a reference surface in model investigations. It is worth noticing (see figure 1) that the droplet tem-

1
2
3 perature is practically constant below the Gibbs surface. Other possible reference surfaces can be
4 defined, however they don't provide easy solution of the surface tension problem.
5
6

7 The analysis presented in this work concentrates on the transfer of mass. The full model de-
8 scribes also the energy transfer.^{4,5,13} The full description is necessary for the system consisting of
9 two or more components, especially when the heat is primarily carried by non-evaporating com-
10 ponent, e.g. in a case of evaporation of water droplets to moist air.^{14,15} In case of one-component
11 system, equations of mass and energy transport are equivalent.
12
13
14
15
16
17

18 19 20 **MD simulation and HK model**

21
22 The MD simulation that we relate to, described in detail in,^{6,7} concerned evaporation of a nano-
23 droplet into its own vapor. A monatomic, Lennard-Jones (LJ) fluid, corresponding to argon was
24 used. The potential representing an LJ atom was truncated for radii larger than 0.875 nm. The LJ
25 diameter was taken as 0.35 nm. Each simulation run started with a liquid droplet equilibrated with
26 surrounding gas and located at the center of a sphere of radius R_b . Gas particles were reflected
27 elastically from the boundary of the sphere. During the evaporation process, the center of the
28 droplet was fixed at the center of the sphere. The parameters of the simulation were selected so
29 that the simulated process was fully self-controlled and only the temperature at R_b was fixed. The
30 number of LJ atoms used in simulations ranged from $\sim 7.5 \times 10^5$ to $\sim 2.7 \times 10^6$ and the droplet
31 temperature found in different simulations ranged from ~ 95 to ~ 150 K. The nano-droplet radius
32 decreased, due to evaporation, from ~ 12 to ~ 3 nm. The studied system can be perceived as
33 consisting of three phases of LJ fluid: droplet core, interface region (droplet surface layer) and
34 surrounding vapor.
35
36
37
38
39
40
41
42
43
44
45
46
47
48
49

50 We start our considerations with a standard HK model and make use of the density and tem-
51 perature profiles from the MD simulation. In general, mass transport from the evaporating droplet
52 can be expressed as
53
54

$$55 \frac{dm}{dt} = -S(j_{out} - j_{in}) , \quad (1)$$

56
57
58
59
60

where m is the droplet mass, j_{out} and j_{in} are the outgoing and ingoing mass fluxes respectively and S is the droplet surface area. The ratio between j_{in} and the mass flux of molecules colliding with the surface j_{col} defines the mass accommodation (condensation) coefficient α_c and reflects the permeability of the interface:

$$\alpha_c = \frac{j_{in}}{j_{col}} . \quad (2)$$

In general, α_c may be expected to be a function of state of the surface phase.¹⁶⁻¹⁸ Combining (1) and (2) we obtain

$$\frac{dm}{dt} = -S(j_{out} - \alpha_c j_{col}) . \quad (3)$$

In the frame of kinetic theory of gases, j_{col} corresponds to the thermal flux in the gas phase for the current state of the system:

$$j_{col} = \frac{\rho_v(T_v)u(T_v)}{4} , \text{ where } u = \sqrt{\frac{8k_B T_v}{\pi m_p}} \quad (4)$$

is the average thermal velocity of molecules in the gas phase, ρ_v and T_v are the density and temperature of vapor respectively, m_p is the mass of molecules (LJ atom in the MD simulation), and k_B is the Boltzman constant. Similarly, classical approach at the micro-scale is based on the assumption that the outgoing flux is a function of temperature only. It is inferred^{4,5} that j_{out} must be equal to the ingoing flux at equilibrium corresponding to T_d :

$$j_{out} = \alpha_{ce} j_{ine} = \alpha_{ce} \frac{\rho_{ve}(T_d)u(T_d)}{4} . \quad (5)$$

The subscript ‘e’ indicates the equilibrium state and we abandon the usual assumption of $\alpha_{ce} = \alpha_c$ (eg.^{5,19}). It remains to be verified, whether these assumptions hold at the nano-scale. It is also worth noting that though the description is valid for both evaporation and condensation it uses only the condensation coefficients.

We notice (see figure 1) that the shape of the fluid density profile in the interfacial region hardly

changes during the evaporation. Thus the left-hand-side of equation 3 can be expressed as

$$\rho_d \frac{dV_d}{dt} + \rho_s \frac{dV_s}{dt}, \quad (6)$$

where V_d and ρ_d are the volume of the droplet core and the bulk liquid density respectively, while V_s and ρ_s are the volume and the effective density of the interface region respectively. As it has been mentioned, it is convenient to adopt the Gibbs surface (sphere) radius as the droplet (surface) radius a . We introduce the droplet core radius as $a - \delta a$ (see figure 1), where $\delta a \simeq const$ defines the cut-off position in the fluid density profile. We chose it to obey the equality $(d\rho/dr)_{r=a-\delta a} = 0.01(d\rho/dr)_{r=a}$, where r is the distance from the droplet center and ρ is the corresponding fluid density. Thus, $dV_d = 4\pi(a - \delta a)^2 da$, $dV_s = 4\pi a^2 da$ and $S = 4\pi a^2$. Therefore, equation 3 can be rewritten in a form describing the evolution of the droplet radius:

$$4 \left[\rho_d \left(\frac{a - \delta a}{a} \right)^2 + \rho_s \right] \dot{a} = \alpha_c(T_s) \rho_v(T_v) u(T_v) - \alpha_{ce}(T_d) \rho_{ve}(T_d) u(T_d). \quad (7)$$

It is natural to link α_c to the droplet surface (Gibbs surface) and the temperature there, hence the notation: $\alpha_c(T_s)$. However, as it has been already mentioned, $T_s \simeq T_d$. The values of ρ_d and T_d were taken as averages of the density and temperature profiles over the droplet core, and ρ_v and T_v as averages over the mean free path at the beginning of the vapor phase. The cut-off radius for the vapor phase R was chosen to obey the equality $(d\rho/dr)_{r=R} = 0.05(d\rho/dr)_{r=a}$. Averaging minimizes the error due to limited number of LJ atoms. Since the mass contained in the droplet core is proportional to a^3 while the mass contained in the transient (interface) region is proportional to $a^2 \delta a$, the term corresponding to interface region can be omitted for the droplet larger than ~ 10 nm.

The value of ρ_{ve} must be estimated from the relation describing the equilibrium state of the system at the temperature T_d . At the micro-scale and macro-scale a good estimation of ρ_{ve} is delivered by the set of three equations: the (extended) Antoine equation (see the Appendix), the Kelvin equation and the van der Waals (or even ideal gas) equation. It turns out that these equations can be applied at the nano-scale as well. In particular, the extended Antoine equation given in²⁰

1
2
3 and the Kelvin equation were verified with the MD simulations⁸ for $a > 3$ nm at the temperature
4 range from ~ 85 K to ~ 105 K.
5
6

7 In order to find ρ_{ve} over the curved surface correctly, the Kelvin equation must be applied. At
8 the nano-scale, a corrected value of the surface tension (as a function of droplet radius) must be
9 used. This value is provided by Tolman formula, which is an approximate solution of the Tolman
10 equation.^{11,12} The Tolman formula fails for droplet radii smaller than ~ 50 nm.⁸ However, using
11 data from,⁸ we found that the Tolman formula can be heuristically modified to accommodate all
12 radii greater than ~ 3 nm. We propose the following improved formula in the Koenig's notation:¹²
13
14
15
16
17
18
19

$$\frac{\gamma(a_{st})}{\gamma_{\infty}} = \left(1 - 2\frac{\delta_T}{a_{st}}\right)^w, \quad (8)$$

20
21 where $\gamma(a_{st})$ is the surface tension at the surface of tension, γ_{∞} is the surface tension of the flat
22 interface, $\delta_T = a - a_{st}$ is the Tolman length, related to the Gibbs surface (droplet) radius a and
23 the radius of the surface of tension a_{st} , and w is the added exponent. The empirical formula for
24 the temperature dependence of γ_{∞} for the LJ liquid was found from^{6,8} (see the Appendix) for
25 the temperature range from ~ 85 K to ~ 135 K. Formula 8 was very satisfactorily fitted to data
26 published in,⁸ yielding $w = 1.6 \pm 0.2$ and $\delta_T = 0.41 \pm 0.06$ nm. So far we can attribute no physical
27 meaning to w parameter.
28
29
30
31
32
33
34
35
36
37
38

39 The value of the condensation coefficient at equilibrium $\alpha_{ce}(T_d)$ as the function of droplet
40 temperature is known from independent MD simulations⁹ (see Appendix) for the temperature
41 range from ~ 70 K to ~ 130 K.
42
43
44

45 Thus, for $a \gtrsim 10$ nm, α_c can remain the only free parameter of the model, while for smaller a ,
46 the effective interface density ρ_s also has to be fitted. Since in our case $a \lesssim 10$ nm for the most part
47 of the evolution, ρ_s was always fitted.
48
49
50
51
52
53
54
55
56
57
58
59
60

Results and discussion

Two examples of a fit of equation 7 to molecular dynamics data are presented in figure 2 in $\dot{a}(a)$ form.

The density and temperature of fluid (used in equation 7) yielded by MD simulation for limited number of (LJ) atoms fluctuate significantly. In consequence, $\dot{a}(t)$ calculated from $a(t)$ fluctuates significantly as well. Thus, 9-points moving average was applied to $\dot{a}(a)$ and the difference between the raw and the averaged \dot{a} served as an estimate of the uncertainty of \dot{a} obtained from MD simulation. Then, the optimization can be performed unambiguously and the quality of fit is good for $a \gtrsim 4$ nm (compare also our results for larger droplets^{14,15}). It proves, that the continuous-medium HK approach can be adopted at the nano-scale. The detailed analysis showed that the approach is applicable as long as the surface layer (interface region) density profile is conserved (which is accompanied by $T_d \simeq const$).

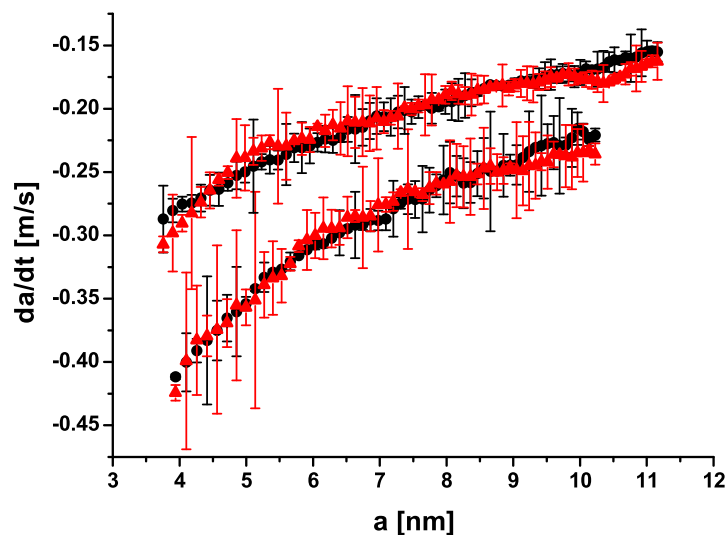


Figure 2: Two examples of nano-droplet evaporation in $\dot{a}(a)$ form (derivative of the droplet radius with respect to time versus the radius); (black) solid dots represent MD data from,⁶ (red) triangles correspond to fits of equation 7.

We present $\alpha_c(T_d)$ and $\alpha_{ce}(T_d)$ in figure 3. $\alpha_c(T_d)$ obtained for different temperatures is self-consistent and consistent with $\alpha_{ce}(T_d)$. It is also generally consistent with previous results at the

micro-scale,^{14,21,22} though the Arrhenius relation is not followed. $\alpha_c(T_d)$ and $\alpha_{ce}(T_d)$ dependence on the liquid temperature T_d are very similar, but $\alpha_c(T_d) < \alpha_{ce}(T_d)$ for all T_d . Such relation seems justified, since α_c is the condensation coefficient for an evaporating droplet. The second parameter of the fit, ρ_s , is presented in figure 4 versus ρ_d . All parameters of the fit are presented in table 1.

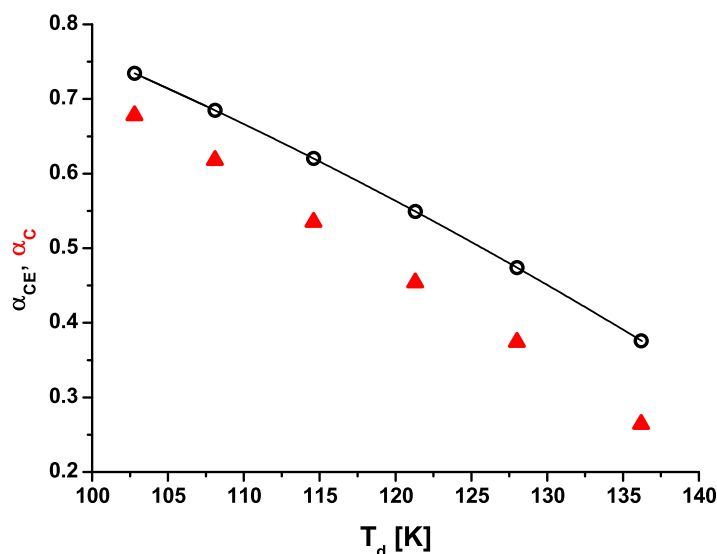


Figure 3: Condensation coefficients, presented versus droplet temperature T_d : (black) open circles and (black) solid line - α_{ce} calculated with equation 5 and ((red) solid triangles) - α_c found as the free parameter of equation 7.

Another parametrization of the fit is also possible. Now we assume that the functional dependence of α_{ce} and α_c upon temperature is the same. By introducing an effective temperature at interface $T_{s(eff)}$ and substituting $\alpha_c = \alpha_{ce}(T_{s(eff)})$ (using equation 11), $T_{s(eff)}$ and ρ_s become the free parameters of the fit. The new parameter $T_{s(eff)}$ of the fit is presented in figure 5 as a function of the liquid temperature T_d .

For engineers applications the free parameters can be totally ruled out from the model, at least far from the critical point, by using linear and quadratic expressions binding them to the corresponding parameters of the droplet: $T_{s(eff)} = 1.068(\pm 0.002)T_d$ and $\rho_s = 25(\pm 0.1) \times 10^{-5} \rho_d^2$ respectively. As far as in real system it would be possible to measure a , T_d and T_v all the parameters of the model can be calculated. However, the coefficients of the above relations must be found by

Table 1: Parameters T_d and δa found from MD simulations; $\alpha_{ce}(T_d)$ calculated with equation 11; α_c , T_s (equivalently) and ρ_s found from the fit of equation 7 to the MD simulations.⁶

	δa	T_d	$\alpha_{ce}(T_d)$	α_c	T_s	ρ_s
	(nm)	(K)			(K)	(kg/m ³)
uncertainty:	± 0.2	± 0.2	± 0.02	± 0.004	± 0.5	± 40
1	1.3	102.8	0.72	0.676	109.4	380
2	1.3	108.1	0.67	0.616	115.3	370
3	1.8	114.6	0.61	0.531	123.4	340
4	1.7	121.3	0.54	0.451	130.6	310
5	1.9	128	0.46	0.366	137	280
6	2.5	136.2	0.36	0.263	145.5	285

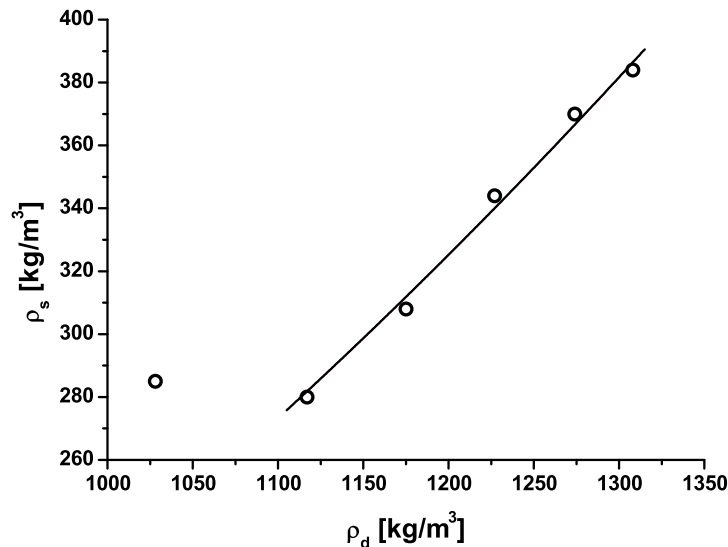


Figure 4: The effective droplet surface density ρ_s , found from fit, versus corresponding droplet core density ρ_d (open circles). Solid line corresponds to quadratic fit (the point closest to the critical temperature was excluded).

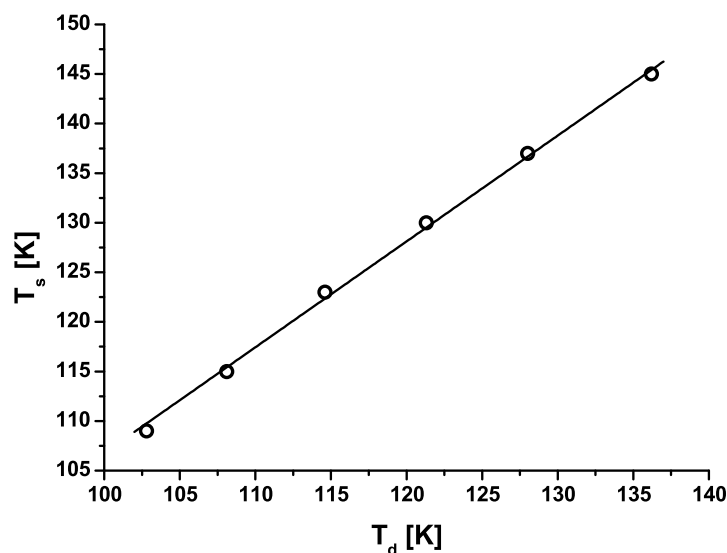


Figure 5: The effective droplet surface temperature T_s found from fit, presented versus droplet core temperature T_d . Solid line corresponds to linear regression.

analyzing the MD simulations.

Summary

We demonstrated that the HK equation can be successfully applied to nano-droplet evaporation for radii larger than ~ 4 nm. We adapted the variables and parameters in the equation to the nano-scale. The surface of the droplet was defined as the Gibbs equimolecular dividing surface and the surface of tension was distinguished. The choice of the Gibbs surface as the main reference surface was verified as beneficial. An empirical modification of the Tolman formula describing the dependence of the surface tension upon interface curvature for droplet radii smaller than ~ 50 nm was proposed to fit MD simulation.⁸ The modified formula holds for radii larger than ~ 3 nm. We assumed that the evaporation coefficient for system in and out of equilibrium may differ. The empirical dependency of the evaporation coefficient of Ar at equilibrium upon temperature in the range from 70 K to 130 K was found from MD simulation.⁸ Similarly, the dependence of the surface tension for flat interface of liquid Ar in Ar gas (at the nano-scale) upon temperature between 85 K

1
2
3 and 130 K was found from data published in references.^{6,8} The Antoine equation for saturation
4 pressure of Ar vapor from²⁰ was verified for temperature range from 85 K to 105 K.
5
6

7 Two parameterizations of the Hertz-Knudsen equation were proposed: (i) one using off-equilibrium
8 condensation coefficient and effective density and (ii) another one using effective density and tem-
9 perature at the interface. Using the first parametrization we reached the conclusion that the con-
10 densation coefficient is indeed a function of the droplet surface temperature only, which makes the
11 condensation coefficient in and out of equilibrium seemingly different. This finding also led to
12 the second parametrization. The second parametrization, in turn, opened way to an approximate
13 solution of the Hertz-Knudsen equation requiring no free parameters. Such solution is suitable
14 for experimental use at the nano-scale if only the temperature of the droplet (core) can be mea-
15 sured. However, such measurements cannot be done with our current apparatus, suitable only for
16 micro-droplet experiments.^{14,15,22}
17
18
19
20
21
22
23
24
25
26
27

28 29 30 **Acknowledgement**

31
32 This work was supported by the Ministry of Science and Higher Education/European Science
33 Foundation (ESF/PESC EPSD program) as a scientific project 2010–2013 and by Polish Ministry
34 of Science and Higher Education under grant No N N202 126837.
35
36
37
38
39
40

41 **Appendix: Empirical formulas used in calculations**

- 42
43
44 1. The extended Antoine equation for the saturated vapor pressure above the flat interface^{8,20}
45 verified for the temperature range from ~ 85 K to ~ 105 K:
46
47

$$48 \ln \frac{p_{sar}}{p_c} = (1 - |t|)^{-1} [a|t| + b|t|^{1.5} + c|t|^3 + d|t|^4], \text{ where } t = \frac{T - T_c}{T_c}. \quad (9)$$

49
50
51
52

53 For Ar: $p_c = 48.7$ bar, $T_c = 150.8$ K and the Antoine coefficients $a = -5.90501$, $b =$
54 1.12627 , $c = -0.76787$, $d = -1.62721$.
55
56
57
58
59
60

- 1
2
3
4
5
6
7
8
9
10
11
12
13
14
15
16
17
18
19
20
21
22
23
24
25
26
27
2. The ‘empirical’ dependence of the surface tension for Argon for flat interface (at equilibrium) as a function of temperature, for the temperature range^{6,8} from ~ 85 K to ~ 135 K is as follows:

$$\gamma_{\infty}(T) = [298(\pm 4) - 2(\pm 0.04)T] \times 10^{-4} . \quad (10)$$

3. The ‘empirical’ dependence of the (equilibrium) mass accommodation coefficient upon the droplet (surface) temperature, found from the data published in reference⁸ for the temperature range from ~ 70 K to ~ 130 K is as follows:

$$\alpha_{ce}(T) = 1.2(\pm 0.01) - 4(\pm 0.1) \times 10^{-5} T^2 . \quad (11)$$

References

- 28
29
30
31
32
33
34
35
36
37
38
39
40
41
42
43
44
45
46
47
48
49
50
51
52
53
54
55
56
57
58
59
60
- (1) Cheng, S.; Lechman, J.; Plimpton, S.; Grest, G. *J.Chem.Phys.* **2011**, *134*, 224704-1-13.
- (2) Babin, V.; Hołyst, R. *J. Phys. Chem. B* **2005**, *109*, 11367-11372.
- (3) Babin, V.; Hołyst, R. *J. Chem. Phys.* **2005**, *123*, 104705.
- (4) Knudsen, M. *The Kinetic Theory of Gases: Some Modern Aspects*; Methuen: London, 1950.
- (5) Pruppacher, H.; Klett, J. *Microphysics of Clouds and Precipitation*; Kluwer: Dordrecht, 1997.
- (6) Hołyst, R.; Litniewski, M. *Phys. Rev. Lett.* **2008**, *100*, 055701-1-4.
- (7) Hołyst, R.; Litniewski, M. *J. Chem. Phys.* **2009**, *130*, 074707.
- (8) Yaguchi, H.; Yano, T.; Fujikawa, S. *Fluid Sci. and Tech.* **2010**, *5*, 180-191.
- (9) Ishiyama, T.; Yano, T.; Fujikawa, S. *Phys. Fluids* **2004**, *16*, 2899-2906.
- (10) Hirschfelder, J.; Curtiss, C.; Bird, R. *Molecular Theory of Gases and Liquids*; Wiley: New York, 1954.

- 1
2
3
4 (11) Tolman, R. *J. Chem. Phys.* **1949**, *17*, 333-337.
5
6
7 (12) Koenig, F. *J. Chem. Phys.* **1950**, *18*, 449-459.
8
9
10 (13) Sirignano, W. *Fluid Dynamics and Transport of Droplets and Sprays*; Cambridge University
11 Press: Cambridge, 2010.
12
13
14 (14) Zientara, M.; Jakubczyk, D.; Kolwas, K.; Kolwas, M. *J. Phys. Chem. A* **2008**, *112*, 5152-
15 5158.
16
17
18 (15) Zientara, M.; Jakubczyk, D.; Derkachov, G.; Kolwas, K.; Kolwas, M. *J. Phys. D* **2005**, *38*,
19 1978-1983.
20
21
22
23
24 (16) Tsuruta, T.; Tanaka, H.; Masuoka, T. *Int. J. Heat Mass Transfer* **1999**, *42*, 4107-4116.
25
26
27 (17) Nagayama, G.; Tsuruta, T. *J. Chem. Phys.* **2003**, *118*, 1392-1399.
28
29
30 (18) Tsuruta, T.; Nagayama, G. *Energy* **2005**, *30*, 795-805.
31
32
33 (19) Fuchs, N. *Evaporation and Droplet Growth in Gaseous Media*; Pergamon: London, 1959.
34
35
36 (20) Reid, R.; Prausnitz, J.; Poling, B. *The Properties of Gases and Liquids*; McGraw-Hill: New
37 York, 1987.
38
39
40 (21) Li, Y.; Zhang, H.; Davidovits, P.; Jayne, J.; Kolb, C.; Worsnop, D. *J. Phys. Chem. A* **2002**,
41 *106*, 1220-1227.
42
43
44
45 (22) Jakubczyk, D.; Derkachov, G.; Do Duc, T.; Kolwas, K.; Kolwas, M. *J. Phys. Chem. A* **2010**,
46 *114*, 3483-3488.
47
48
49
50
51
52
53
54
55
56
57
58
59
60

